

## Lamb wave-based damage imaging method for damage detection of rectangular composite plates

Pizhong Qiao\* and Wei Fan<sup>a</sup>

Department of Civil and Environmental Engineering, Washington State University, Sloan 117, Pullman, WA, 99164-2910, USA

(Received April 21, 2014, Revised August 23, 2014, Accepted October 24, 2014)

**Abstract.** A relatively low frequency Lamb wave-based damage identification method called damage imaging method for rectangular composite plate is presented. A damage index (*DI*) is generated from the delay matrix of the Lamb wave response signals, and it is used to indicate the location and approximate area of the damage. The viability of this method is demonstrated by analyzing the numerical and experimental Lamb wave response signals from rectangular composite plates. The technique only requires the response signals from the plate after damage, and it is capable of performing near real time damage identification. This study sheds some light on the application of Lamb wave-based damage detection algorithm for plate-type structures by using the relatively low frequency (e.g., in the neighborhood of 100 kHz, more suitable for the best capability of the existing fiber optic sensor interrogator system with the sampling frequency of 500 kHz) Lamb wave response and a reference-free damage detection technique.

**Keywords:** damage detection; Lamb wave; composite plates; piezoelectric sensors and actuators; damage imaging

### 1. Introduction

Many structures or their major components in aerospace, civil and mechanical engineering are plate-like structures. Since the failure of these structures may lead to catastrophic economic and human life loss, it is essential to monitor the health of these structures regularly to prevent potential failures. A reliable and effective non-destructive damage detection method is crucial to maintain safety and integrity of these structures.

Lamb waves are elastic waves propagating inside a thin plate with parallel free boundaries. They are widely acknowledged as one of the most promising tools for damage detection in composite structures. Many techniques have been developed to detect and localize damage in beam or plate structures using Lamb wave propagation. Different features of the Lamb wave propagation have been investigated for damage detection such as time of flight (Lestari and Qiao 2005), amplitude attenuation (Tan *et al.* 1995), and mode conversion (Lemistre and Balageas 2000). For simple beam-type of structures, the pitch-catch and pulse-echo experiments perform

---

\*Corresponding author, Professor, E-mail: [Qiao@wsu.edu](mailto:Qiao@wsu.edu)

<sup>a</sup>Former Ph.D. student

well in detection of damage. The pitch-catch method detects damage from the changes in Lamb wave between healthy and damaged structures using a actuator/sensor pair; while the pulse-echo method detects damage from the Lamb wave signal reflected from the damaged region, and it uses one sensor to capture both the excitation and reflection signals.

For plate-type of structures, more sophisticated Lamb wave-based methods are developed to solve the 2-D problem. One type of the widely investigated methods is the time reversal method. The time reversal method was developed by Fink *et al.* (1992) and Fink (1992) in connection with the pitch-catch method. According to the time reversal concept, an input signal can be reconstructed at an excitation point if an output signal recorded at another point is reemitted to the original source point in a time-reversed fashion. This process is referred to as the time-reversibility of waves. Recently, the time reversal method has been reported in structural health monitoring (SHM) by several authors. Wang *et al.* (2004) used an experimental and theoretical investigation of the influence of dispersion Lamb wave on temporal and spatial focusing of time-reversal waves in plates. A synthetic time-reversal array method was proposed to improve the SNR of the testing, and an imaging method was used to locate damage and approximate its size. Sohn *et al.* (2007) and Park *et al.* (2007) used the wavelet signal processing technique to enhance the time reversibility of Lamb wave in composite plates. This enhanced method is able to detect damage without relying on baseline data. The validity of the proposed method was exemplified through the experimental studies on a quasi-isotropic laminate with delamination.

Another type of the widely investigated methods is the phased array methods in connection with the pulse-echo method. The principles of ultrasonic phased array methods resemble that of phased array used in radar, sonar, seismology and medical imaging. Phased array is a group of actuators/sensors with distinct spatial distribution, in which the relative phase of the actuators/sensors can be varied algorithmically to control the effective propagation/sensing direction of the array. The backscattered Lamb wave signals from damaged area can be analyzed to obtain damage index for damage identification. Deutsch *et al.* (1997) developed a self-focusing phased array for the Lamb wave inspection of thin plates. The time delays from the first transmission test are used to adjust the times of excitation of the elements for transmission focusing on the defect. Experimental results demonstrated the ability to self-focus on single defects. For multiple defects, the technique has been extended to focus on the defect that produces the largest backscattered signal. Wilcox (2003) presented an omni-directional guided wave array transducers that contain a circular pattern of elements individually behaving as omni-directional point transmitters or receivers. A phased addition algorithm was developed that allows an omni-directional, B-scan image of the surrounding plate to be synthesized from any geometry of array. Experimental data obtained from a guided wave array for exciting and detecting the S0 Lamb wave mode in a 5-mm thick aluminum plate were processed with both algorithms, and the results were discussed. Giurgiutiu *et al.* (2002, 2003) and Yu and Giurgiutiu (2008) developed a generic beamforming algorithm called the embedded ultrasonics structural radar (EUSR) for in-situ structural health monitoring of thin-wall structures using the embedded piezoelectric-wafer active-sensors (PWAS). The experiments showed that the direct monitoring of crack growth could be achieved with the PWAS using the EUSR algorithm. There are also other types of damage identification methods based on Lamb wave in the literature, such as Lamb wave tomography (Jansen and Hutchins 1992, Leonard *et al.* 2002, Hay *et al.* 2006, Sekhar *et al.* 2006) and migration technique (Lin and Yuan 2001, Muralidharan *et al.* 2008).

In order to obtain clear Lamb wave signal for damage detection analysis, most of above mentioned methods need meet the high frequency requirements, i.e., the excitation signal must

operate in high frequency range (typically in form of a windowed tone burst) so that the incident signal and the boundary/defect reflected signal will not overlap each other. However, testing in a high frequency range usually requires high cost and bulky signal generation and data acquisition system. Therefore, it is often difficult to make a cost-effective and portable damage detection system based on these high frequency Lamb wave-based methods.

In this study, a low frequency Lamb wave-based damage detection method is proposed for detecting delamination in rectangular composites plates. In particular, the fundamental anti-symmetric  $A_0$  Lamb wave propagation in the composite plates at the frequencies around 50 kHz is monitored by a smart piezoelectric sensor/actuator network with only a single actuator and a few sensors. A damage index is proposed to identify the delamination based on the time of flight (TOF) of the incident wave and the boundary reflected wave after interacting with delamination. The rest of the paper is organized as follows. The fundamentals of Lamb wave is briefly introduced in Section 2. The application of the low frequency Lamb wave in damage detection is demonstrated using a numerical plate model in Section 3. The effectiveness and applicability of the proposed method is validated in Section 4 via an experimental program using surface-bonded PZT (Lead Zirconate Titanate) actuator/sensor.

## 2. Fundamentals of Lamb wave

A Lamb wave exists in a plate usually in the form of a superposition of multiple Lamb wave modes. A Lamb wave mode can be either symmetric or anti-symmetric. Its dispersion relations in a homogeneous isotropic plate can be calculated using the well-known Rayleigh-Lamb frequency relations.

$$\frac{\tan(qh)}{\tan(ph)} = -\frac{4k^2 pq}{(q^2 - k^2)^2} \quad \text{for symmetric modes} \quad (1)$$

$$\frac{\tan(qh)}{\tan(ph)} = -\frac{(q^2 - k^2)^2}{4k^2 pq} \quad \text{for antisymmetric modes} \quad (2)$$

$$p^2 = \frac{\omega^2}{c_L^2} - k^2, q^2 = \frac{\omega^2}{c_T^2} - k^2, k = \frac{\omega}{c_P}, \quad (3)$$

where  $h, k, \omega, c_L, c_T, c_P$  denote the plate thickness, wave number, circular frequency, longitudinal wave velocity, transverse wave velocity, and phase velocity, respectively.

It should be noted that the above equations can be solved only by numerical methods, although they look simple. The dispersion curves for isotropic aluminum material are presented in Fig. 1. As shown in Fig. 1, it should be noted that at the relatively low frequency range, the dispersion curves of the fundamental symmetric and anti-symmetric Lamb wave mode converge to the axial wave and flexural plate wave solution from Love-Kirchhoff plate theory, respectively. The Lamb wave propagation investigated in this study is focused in this low frequency range.

For laminated fiber-reinforced composite plates, the solution is more complicated since it should satisfy the Christoffel equation for each layer, the continuity condition at the interfaces and the traction-free boundary conditions at the plate surfaces. The solutions for dispersion relation of multi-layered composite plates by the global matrix method can be found in the literature (Kundu

2004). The carbon fiber-reinforced plastic (CFRP) composite plate considered in this study is a  $[0/90]_4$  carbon/epoxy composite laminate with thickness of 1.78 mm,  $E_{\text{carbon}} = 235.0$  GPa,  $E_{\text{epoxy}} = 3.4$  GPa,  $V_f = 55\%$ . The corresponding dispersion curves at  $0^\circ$  and  $45^\circ$  and comparison between the theoretical and experimental dispersion curves are given by Yang and Qiao (2005), as shown in Fig. 2.

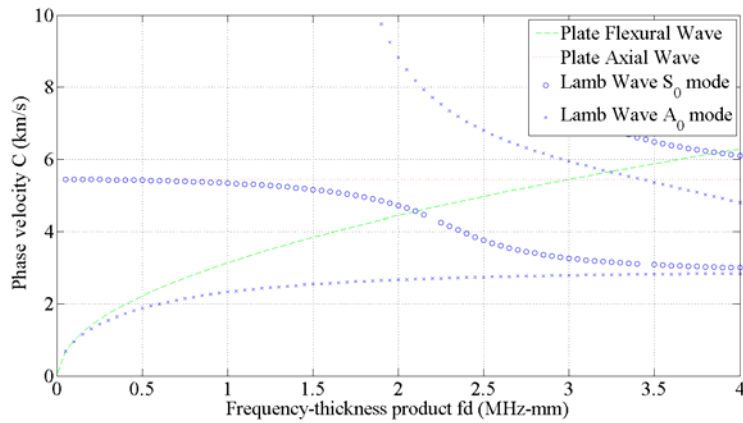
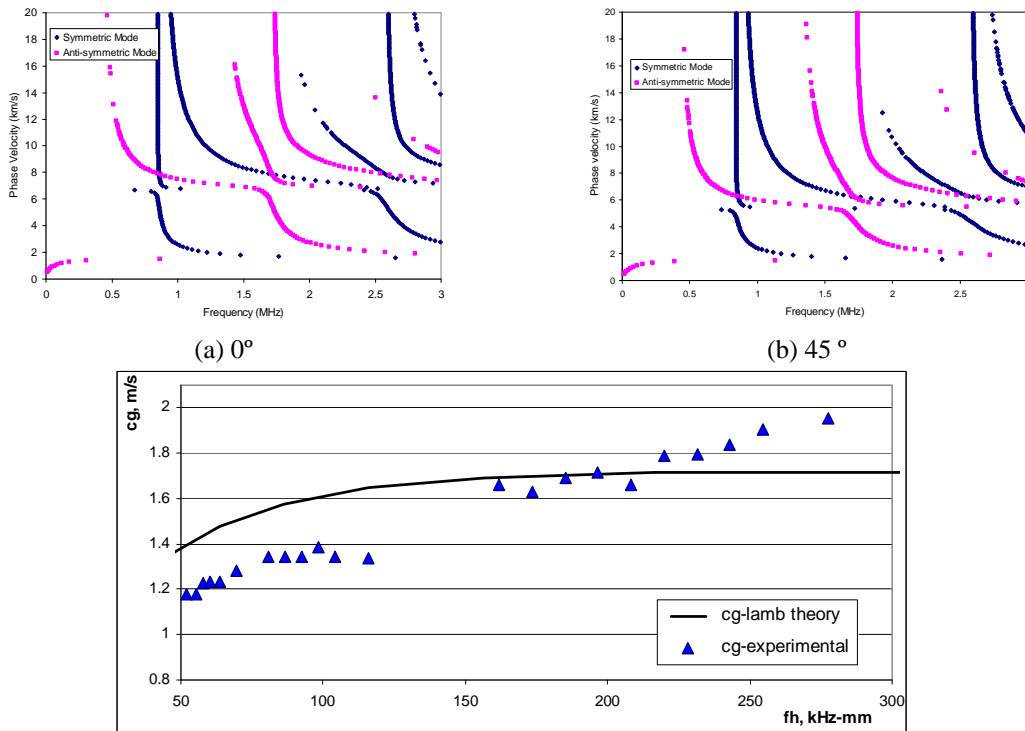


Fig. 1 Dispersion curves for alumina



(c) Comparison between the theoretical and experimental dispersion curve ( $A_0$  mode)

Fig. 2 Dispersion curves for the carbon/epoxy laminated composites

### 3. Low frequency Lamb wave-based damage imaging method

To demonstrate the damage imaging method, two rectangular CFRP composite plates are investigated in this study, one with a localized delamination, and the other as healthy. The dimensions of the plates and the delamination are shown in Fig. 3. Both the plates are  $[0/90]_4$  carbon/epoxy composite laminates with thickness of 1.78 mm,  $E_{\text{carbon}} = 235.0$  GPa,  $E_{\text{epoxy}} = 3.4$  GPa,  $V_f = 55\%$ , the same as described in Section 2. The bottom layer of the damaged plate is delaminated in an area of 36 mm $\times$ 40 mm, as shown in Fig. 3. A PZT actuator is installed at the center of the plate to generate the omni-directional Lamb wave, and four PZT sensors are installed at four corners to capture the Lamb wave signal. A tone burst signal with 3.5 cycles of 50 kHz sine wave is sent by the actuator to excite the  $A_0$  mode Lamb wave. The response is collected by four sensors. It should be noted that it is difficult to generate a pure single mode  $A_0$  Lamb wave in a plate due to the multi-mode nature of Lamb wave. When the plate is excited at the frequency below the cutoff frequency of  $A_1$  mode, the  $A_0$  and  $S_0$  mode lamb wave always co-exist inside a plate. However, using the frequency-tuning technique, it is possible to maximize the amplitude ratio between the  $A_0$  and  $S_0$  mode so that the  $S_0$  mode Lamb wave can be negligible in response signal. This is the case in the low frequency Lamb wave since the  $A_0$  mode will dominate in terms of amplitude at the low frequency range.

When the PZT sensors are adopted as sensors, a pattern of multiple reflections of Lamb wave can be captured. The propagation path of the Lamb wave signal captured by four sensors can be analyzed using a mirror image containing 25 adjacent plates, as shown in Fig. 4.

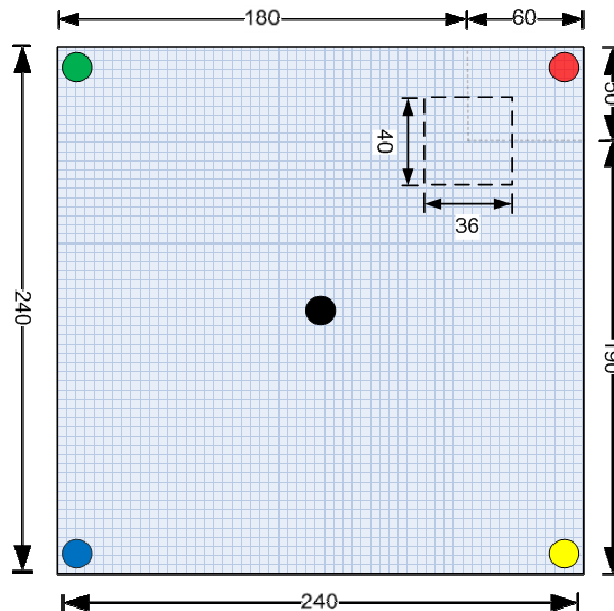
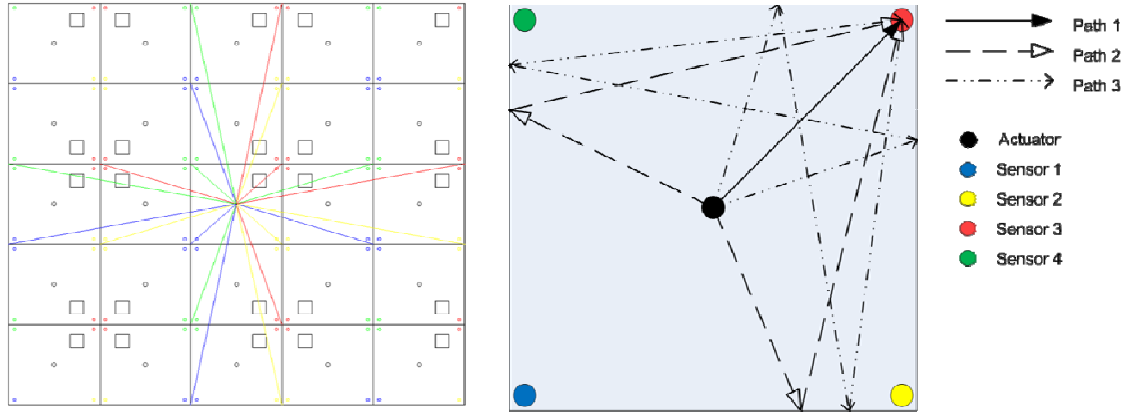


Fig. 3 The dimensions of the plates and the delamination



(a) Mirror image of the original plate

(b) The first three propagation paths of the response signal captured by sensor 3

Fig. 4 Lamb wave propagation paths in the CFRP composite plate

### 3.1 Numerical simulation of wave propagation and delay matrix formulation

The commercial Finite Element Analysis package ABAQUS is used to conduct a dynamic analysis to simulate the Lamb wave propagation. The plate is uniformly divided into 4-node first-order plate elements S4 of size  $2 \text{ mm} \times 2 \text{ mm}$ . The elements have six degrees of freedom at each node. For comparison, both the healthy plate and delaminated plate are modeled. The delamination part of the plate is modeled by two separate sub-plates stacking together: one with the bottom 2 layers of the original plate, and the other with the rest six layers of the plate.

To obtain the wave excitation in the finite element analysis, the excitation applied by the PZT actuators is simulated as the prescribed displacement at the central node of the plate in the out-of-plane direction. The detection of the elastic waves follows the similar principle applied to wave generation. A tone burst signal is sent by the actuator to excite the  $A_0$  mode lamb wave, as shown in Fig. 5. The excitation tone burst signal is a 3.5 cycles of 50 kHz sine wave windowed by a hanning window. The signal can be expressed as follows

$$S(t) = 0.5(1 - \cos(2\pi t \times 50 \times 10^3 / 3.5)) \times \sin(2\pi t \times 50 \times 10^3), 0 \leq t \leq 70 \times 10^{-6} \quad (4)$$

For the dynamic wave finite element analysis (FEA), the time step and element size are the two important factors which decide the accuracy of the FEA. In this study, the time steps of  $10^{-6}$  s are chosen for 50 kHz  $A_0$  mode wave simulation so that the sampling frequency can reach as high as 20 times of the central frequency of the Lamb wave, which is enough to capture the accurate waveform of 100 kHz. The size of the elements (Fig. 6) is chosen as  $2 \text{ mm} \times 2 \text{ mm}$ , which is much smaller than the wavelength of the  $A_0$  wave (about 18.0 mm). Fig. 2(c) shows the comparison between the theoretical and experimental dispersion curves for the  $A_0$  mode in carbon/epoxy composite plate.

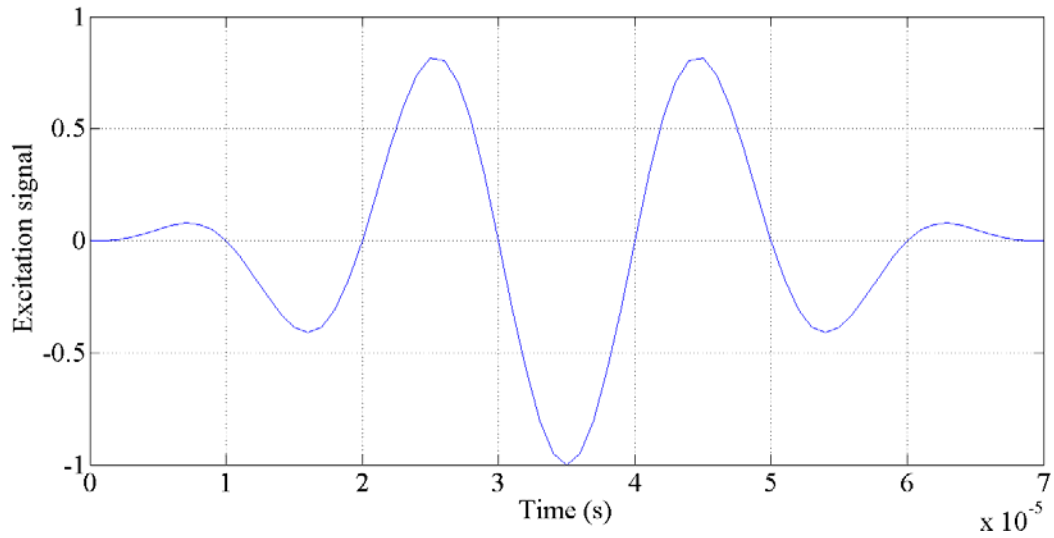


Fig. 5 50 kHz 3.5 cycles Hanning windowed tone burst

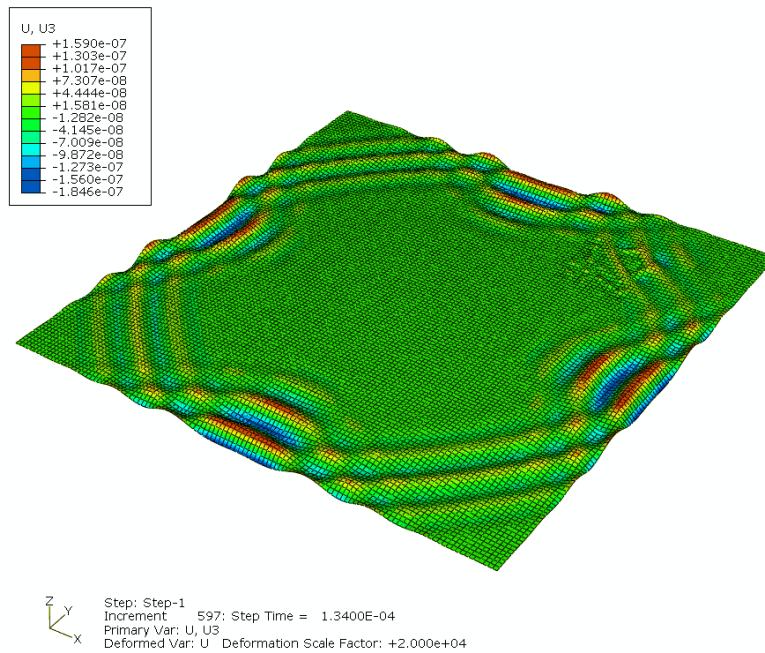


Fig. 6 FE simulation of Lamb wave propagation in the delaminated plate (Deformation Scale Factor = 200,000)

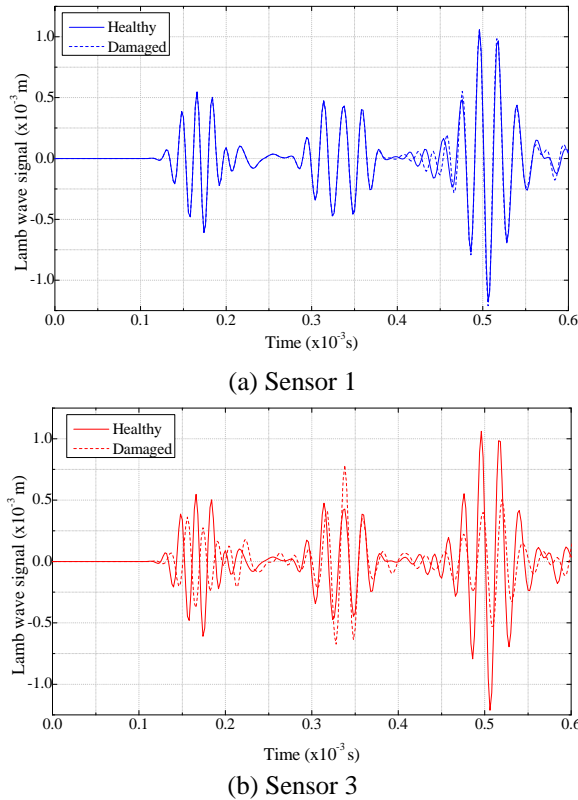


Fig. 7 Lamb wave response signals comparison in the healthy and damaged states by FEA

The finite element simulation of the Lamb wave propagation in the delaminated composite plate is shown in Fig. 6. The comparisons of Lamb wave response in the healthy and damaged states for sensors 1 and 3 are shown in Fig. 7. Three wave packages can be identified in the first  $0.6 \mu\text{s}$  from each signal, corresponding to the first three wave propagation paths. For sensor 1, the response signals in healthy state and damaged state are almost identical; while for sensor 3, the response signals in two states show discrepancies both in amplitude and phase. Although there is substantial damage-induced change in amplitude of the signals, this study will only focus on the time delay of the signal because the time of travel can be measured more accurately in experimental test, while the amplitude of the signals may vary due to the different bonding conditions of the PZT sensors. It can be noticed that for every wave path that passes the delamination area, the corresponding wave package will be delayed in phase because at low frequency range the  $A_0$  wave is very dispersive, a slight loss of stiffness in the delaminated area leads to substantial change in phase velocity. Furthermore, the delay in each wave package is related to the distance that the wave propagates in the delamination area: the longer the wave propagates in the delamination area, the larger the delay in phase. For example, for sensor 3 the wave package 1 is delayed for almost half cycle since the wave path 1 passes through the delamination area, while the wave packages 2 and 3 are only slightly delayed since the wave paths 2 and 3 tip the edge of the area.

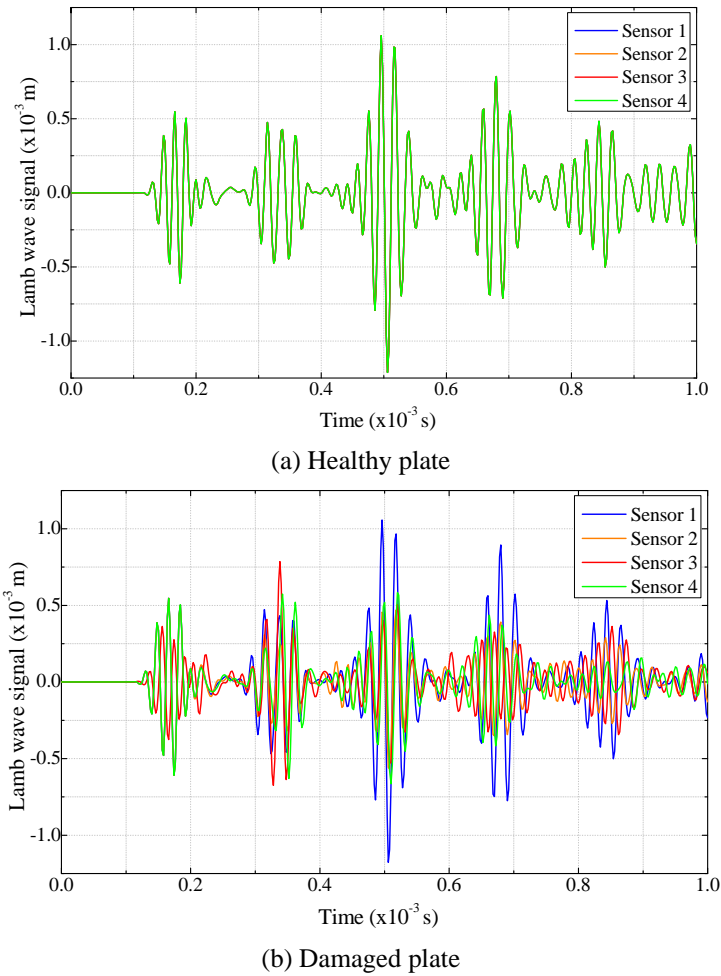


Fig. 8 Lamb wave response signals from FEA

The response signals captured in the healthy and damaged states from all the four corner sensors are summarized in Fig. 8. In the healthy state, the response signals captured in all the four sensors are identical as expected, because they are located symmetrically at four corners. In the damaged state, a pattern of delay in phase can be identified for different sensors in each wave package. From Fig. 8, a delay matrix  $\tau(i, j)$  is defined as the time of delay of sensor  $i$  from the first arrival package in the wave package  $j$  for future damage identification. The delay matrix  $\tau(i, j)$  can be accurately obtained by the following algorithm:

- (1) Hilbert-transform is applied to each response signal curve to obtain the envelope of the signal. From the envelope of the signal, the duration of each wave package (corresponding to each wave propagation path) can be identified using a threshold value, e.g., 10% of the peak amplitude of the wave package.

- (2) In each wave package, responses from different sensors are compared to find the sensor with the first arrival signal and the time of delay for all other sensors. The estimate of the delay between the wave packages from two sensors can be estimated via the cross-correlation technique.
- (3) The estimated delay of sensor  $a$  in wave package  $b$  is collected in the delay matrix  $\tau_1(i, j)$ , where  $i \leq M$ ,  $j \leq N$ ,  $M$  denotes the total number of the sensors, and  $N$  denotes the total number of the wave package/propagation path under investigation.

The delays from each wave package are offset by the mean value of the delays in the package so that the mean value of delays in each package equals zero. Finally, the delay matrix  $\tau(i, j)$

can be obtained by  $\tau(i, j) = \tau_1(i, j) - \frac{1}{M} \sum_{i=1}^M \tau_1(i, j)$ .

### 3.2 Damage imaging method

In this study, a damage imaging method is proposed for damage detection by analyzing the delay matrix  $\tau(i, j)$ . Based on a single damage (delamination) assumption, a damage index ( $DI$ ) can be constructed at an arbitrary location  $C(x, y)$  as follows

$$DI(x, y) = \sum_{i=1}^M \sum_{j=1}^N \tau(i, j) \times \exp[-d_j^2 / s^2] - \sum_{j=1}^N \tau(i, j) \times \exp[-d_i^2 / s^2] \quad (5)$$

where  $x, y$  are the coordinates of the arbitrary location  $C$ ;  $d_i$  denotes the distance from point  $C(x, y)$  to sensor  $i$ ;  $d_j$  denotes the shortest distance from point  $C$  to path  $j$ ;  $s = 2\lambda$ ,  $\lambda$  denotes the wavelength of the incident wave.  $M$  is the total number of sensors; and  $N$  is the total number of wave packages (paths) under investigation. It should be noted that the parameter  $s$  is chosen as  $2\lambda$  because the numerical simulations show that the Lamb wave propagation is most sensitive to damage with dimensions comparable to  $2\lambda$  and ineffective to detect damage with dimensions much smaller than  $\lambda$ .

In Eq. (5), the first term represents the distance of the point  $C$  from path  $j$  weighted by the delay matrix so that the intersection of the delayed paths will be highlighted by the proposed damage index. The second term is introduced to compensate the concentration of damage index at sensor location since sensor locations are always the intersections of  $N$  wave propagation paths. The damage index  $DI$  can be directly used as the illumination value to visualize the damage detection result.

The steps of the damage imaging method are listed as follows

- (1) Collect Lamb wave response signals from sensors;
- (2) Detect the delay matrix  $\tau$ ;
- (3) Calculate the damage index  $DI$  for the whole plate;
- (4) Visualize the damage index  $DI$  for damage identification.

### 3.3 Application of damage imaging method on numerical simulation data

A program based on MATLAB is developed to realize the damage imaging method. The

program is applied to the numerically simulated Lamb wave response data for damage detection. The wavelength of the propagating Lamb wave can be directly measured as  $\lambda = 17$  mm from the simulation data. The damage index  $DI$  generated by the program is then visualized as in Fig. 9(a) and 9(b). It is shown in Fig. 9 that the damage indices for the healthy plate equal to zero, while the damage indices for damaged plate are high in the delaminated area but low in the rest of the plate. Hence, the delamination area in the damaged plate can be highlighted by visualizing  $DI$  in the whole plate. Furthermore, a threshold value of  $DI$  (e.g.,  $DI = 4 \times 10^{-6}$ ) can be set to indicate whether there is a delamination in the plate and approximate the area of delamination.

To verify this method, another similar case study with a different delamination area is conducted based on the FE simulation. The damage index results are shown in Fig. 9(c). It can be concluded from the numerical simulation result that (1) the damage index  $DI$  can correctly indicate the location of the delamination and approximate the damaged area; (2) the damage index  $DI$  will not give a false indication of damage for a healthy plate.

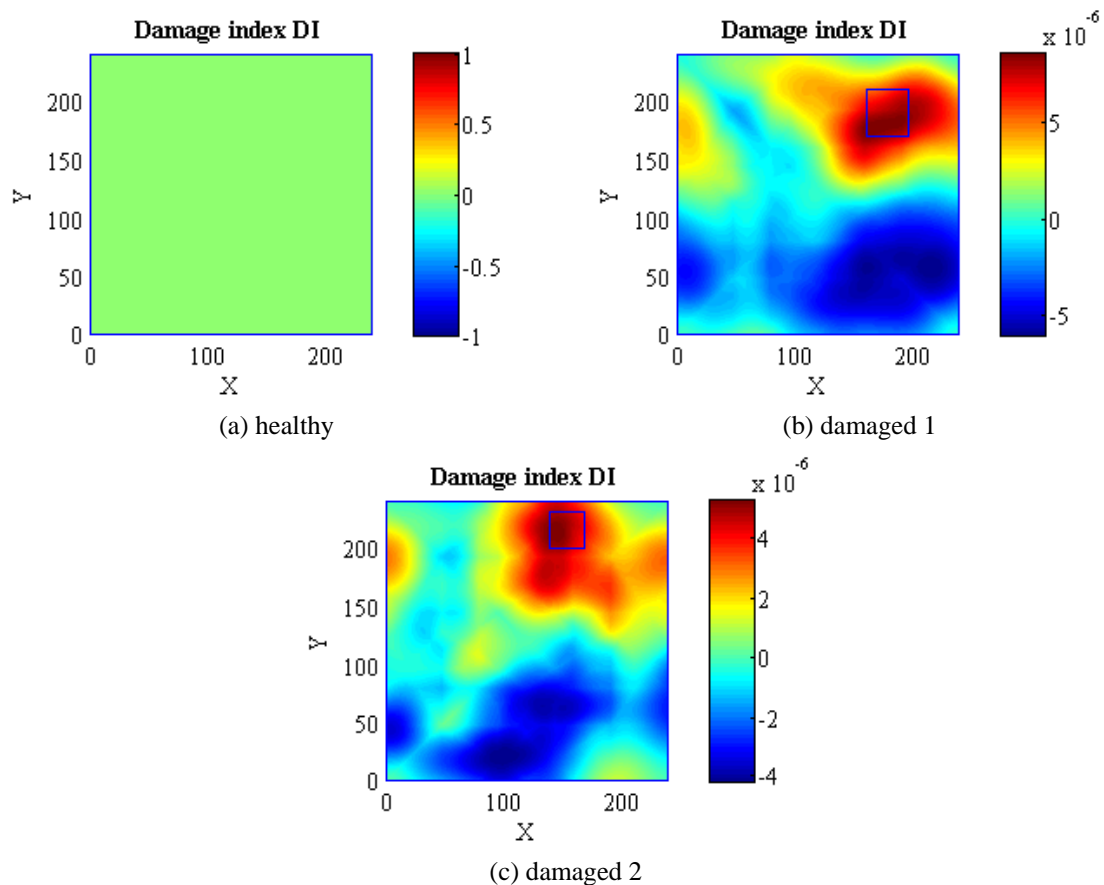


Fig. 9 Damage index generated from the numerical simulation data

## 4. Experimental verification of damage imaging method

### 4.1 Experimental setup

To further verify the low-frequency Lamb-wave-based damage imaging method, two rectangular CFRP composite plates with a size of 240 mm  $\times$  240 mm manufactured by Honeywell International Inc. were experimentally tested in laboratory, one with localized delamination, and the other as intact (healthy). The plates are hanged with elastic strings at one side to simulate a free boundary condition. A delamination with an approximate size of 40 mm  $\times$  36 mm (the same as damaged 1 in Fig. 9(b)) is artificially-induced in the damaged plate by inserting a thin Teflon film between the first and the second layer during manufacturing.

The Lamb wave propagation tests are conducted using one circular PZT actuator with diameter of 12 mm and four square PZT sensors with side length of 8 mm. An Agilent 33120A function generator is adopted to generate the tone burst excitation signal as described in Eq. (4). A Mide Quickpack power amplifier is used to amplify the excitation signal in order to drive the PZT actuator. A HP 54603B oscilloscope is used to capture the response signal generated by the PZT sensors at the sampling frequency of 500 kHz. The captured response signal data is then transmitted into a computer laptop for damage detection. The experimental setup is shown in Fig. 10. The signals from healthy and damaged plate are shown in Fig.11.

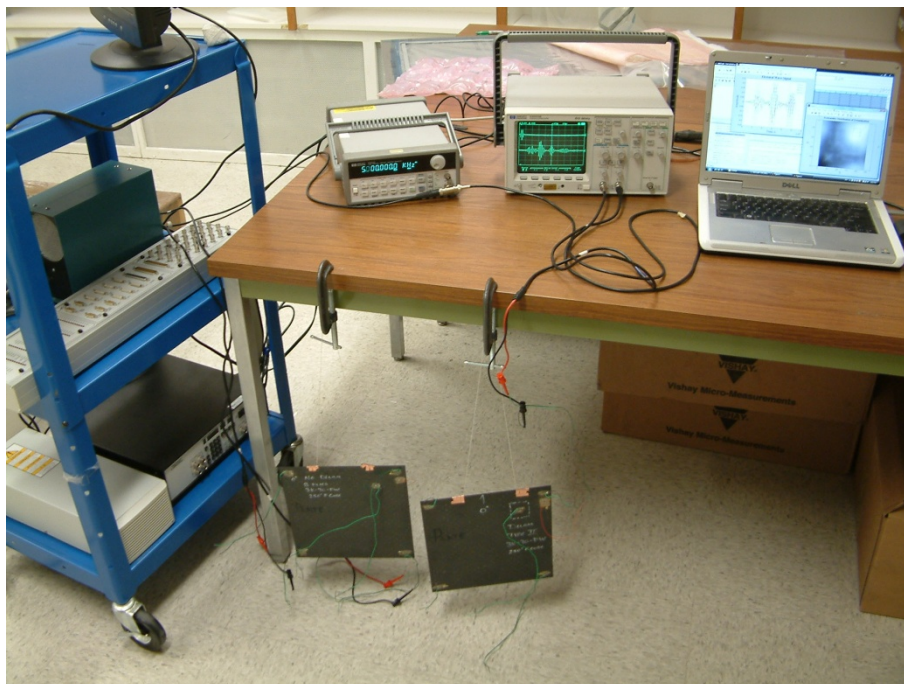
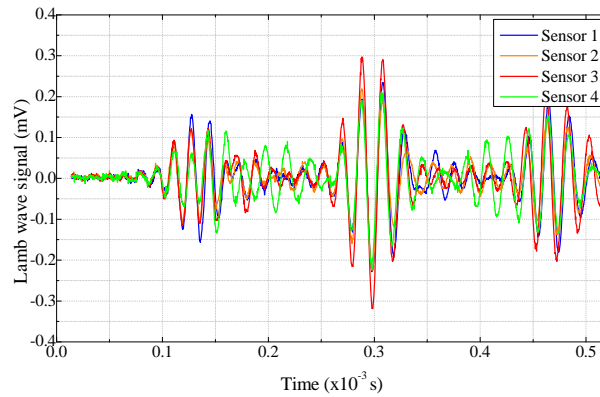
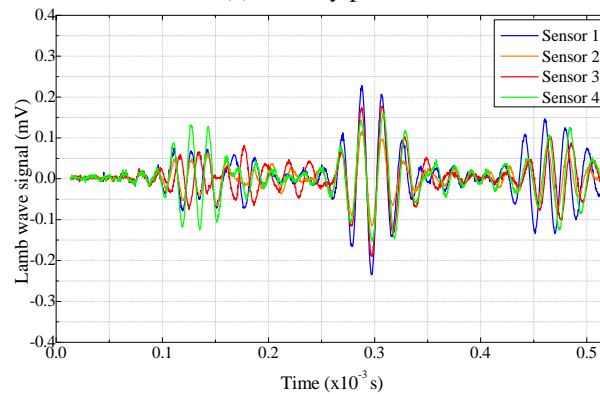


Fig. 10 Experimental setup



(a) Healthy plate



(b) Damaged plate

Fig. 11 Lamb wave response signals from the experimental test

#### 4.2 Application of damage imaging method on experimental test data

The damage imaging method program is applied to the experimentally obtained Lamb wave response data for damage detection. The wavelength of the propagating Lamb wave is assumed to be same as predicted by the numerical simulation. The damage index  $DI$  generated by the program is then visualized as in Fig. 12. It is shown in Fig. 12 that the damage indices show the same pattern as shown in Fig. 9. For the healthy plate,  $DI$  are very low ( $<2 \times 10^{-6}$ ) all over the plate; while for the damaged plate  $DI$  are high in the delaminated area ( $>5 \times 10^{-6}$ ) but low in the rest of the plate. Hence, the delamination area in the damaged plate can be identified by setting an appropriate threshold value of  $DI$  (e.g.,  $DI = 4 \times 10^{-6}$ ).

It can be concluded from the experimental result that (1) the damage index  $DI$  generated by the damage imaging method using the laboratory test data can correctly indicate the location of the delamination and approximate the damaged area; and (2) with an appropriate threshold value, the damage index  $DI$  will not give a false indication of damage for a healthy plate using laboratory test data.

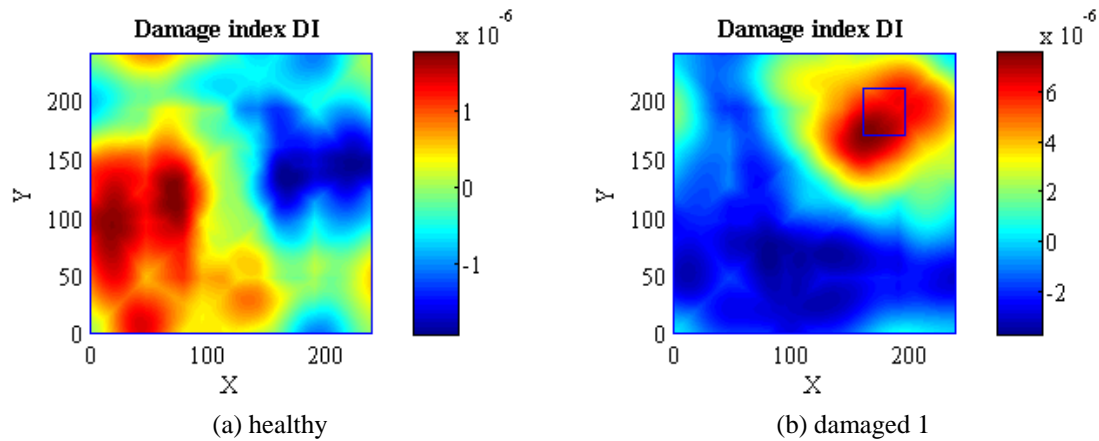


Fig. 12 Damage index generated from the experimental test

## 5. Conclusions

A low frequency Lamb wave-based damage identification method called the damage imaging method is presented. A damage index  $DI$  is generated from the delay matrix of the Lamb wave response signals to indicate the location and approximate area of the damage. The viability of this method is demonstrated by analyzing the numerical and experimental Lamb wave response signals from the composite plates. The proposed method is a response-based, reference-free, and near real time damage detection technique which only requires the response signals from the plate after damage.

This study sheds some light in the application of Lamb wave-based damage detection algorithm for plate-type structures. However, more experiments are needed to demonstrate the practicality of this method for plates with other boundary conditions. The exploration of this method for damage quantification should be the subject of future research.

## Acknowledgements

This study is partially supported by the Alaska University Transportation Center (AUTC) (Contract/Grant No.: DTRT06-G-0011) on Smart FRP Composite Sandwich Bridge Decks in Cold Regions and the NASA STTR (Proposal No.: 08-1 T2.01-9951) on Structural Health Monitoring with Fiber Bragg Grating (FBG) sensor and Piezo-actuator Arrays.

## References

- Deutsch, W.A.K., Cheng, A. and Achenbach, J.D. (1997), "Self-focusing of Rayleigh waves and lamb waves with a linear phased array", *Res. Nondestruct. Eval.*, **9**(2), 81-95.
- Fink, M. (1992), "Time-reversal of ultrasonic fields .1. basic principles", *IEEE T. Ultrason. Ferr.*, **39**(5), 555-566.

- Giurgiutiu, V., Bao, J. and Zhao, W. (2003), "Piezoelectric wafer active sensor embedded ultrasonics in beams and plates", *Exp. Mech.*, **43**(4), 428-449.
- Giurgiutiu, V., Zagrai, A. and Bao, J.J. (2002), "Embedded active sensors for in-situ structural health monitoring, of thin-wall structures", *J. Pressure Vessel Technol. T. - ASME*, **124**(3), 293-302.
- Hay, T.R., Royer, R.L. Gao, H.D., Zhao, X. and Rose, J.L. (2006), "A comparison of embedded sensor Lamb wave ultrasonic tomography approaches for material loss detection", *Smart Mater. Struct.*, **15**(4), 946-951.
- Jansen, D.P. and Hutchins, D.A. (1992), "Immersion tomography using Rayleigh and Lamb waves", *Ultrasonics*, **30**(4), 245-254.
- Kundu, T. (2004), *Ultrasonic Nondestructive Evaluation: Engineering and Biological Material Characterization*, Boca Raton: CRC Press LLC.
- Lemist, K.R., Malyarenko, E.V. and Hinders, M.K. (2002), "Ultrasonic Lamb wave tomography", *Inverse Probl.*, **18**(6), 1795-1808.
- Lemistre, M. and Balageas, D. (2001), "Structural health monitoring system based on diffracted Lamb wave analysis by multiresolution processing", *Smart Mater. Struct.*, **10**(3), 504-511.
- Lestari, W. and Qiao, P.Z. (2005), "Application of wave propagation analysis for damage identification in composite laminated beams", *J. Compos. Mater.*, **39**(22), 1967-1984.
- Lin, X. and Yuan, F.G. (2001), "Damage detection of a plate using migration technique", *J. Intel. Mat. Syst. Str.*, **12**(7), 469-482.
- Muralidharan, A., Balasubramaniam, K. and Krishnamurthy, C.V. (2008), "A migration based reconstruction algorithm for the imaging of defects in a plate using a compact array", *Smart Struct. Syst.*, **4**(4), 449-464.
- Park, H.W., Sohn, H., Law, K.H. and Farrar, C.R. (2007), "Time reversal active sensing for health monitoring of a composite plate", *J. Sound Vib.*, **302**(1-2), 50-66.
- Sekhar, B.V.S., Balasubramaniam, K. and Krishnamurthy, C.V. (2006), "Structural health monitoring of fiber-reinforced composite plates for low-velocity impact damage using ultrasonic lamb wave tomography", *Struct. Health Monit.*, **5**(3), 243-253.
- Sohn, H., Park, H.W., Law, K.H. and Farrar, C.R. (2007), "Damage detection in composite plates by using an enhanced time reversal method", *J. Aerospace Eng.*, **20**(3), 141-151.
- Tan, K.S., Guo, N., Wong, B.S. and Tui, C.G. (1995), "Experimental evaluation of delaminations in composite plates by the use of Lamb waves", *Compos. Sci. Technol.*, **53**(1), 77-84.
- Wang, C.H., Rose, J.T. and Chang, F.K. (2004), "A synthetic time-reversal imaging method for structural health monitoring", *Smart Mater. Struct.*, **13**(2), 415-423.
- Wang, C.H., Rose, J.T. and Chang, F.K. (2004), "A synthetic time-reversal imaging method for structural health monitoring", *Smart Mater. Struct.*, **13**(2), 415-423.
- Wilcox, P.D. (2003), "Omni-directional guided wave transducer arrays for the rapid inspection of large areas of plate structures", *IEEE T. Ultrason. Ferr.*, **50**(6), 699-709.
- Wu, F., Thomas, J.L. and Fink, M. (1992), "Time-reversal of ultrasonic fields .2. experimental results", *IEEE T. Ultrason. Ferr.*, **39**(5), 567-578.
- Yang, M.J. and Qiao, P.Z. (2005), "Modeling and experimental detection of damage in various materials using the pulse-echo method and piezoelectric sensors/actuators", *Smart Mater. Struct.*, **14**(6), 1083-1100.
- Yu, L. and Giurgiutiu, V. (2008), "In situ 2-D piezoelectric wafer active sensors arrays for guided wave damage detection", *Ultrasonics*, **48**(2), 117-134.